Repository Istituzionale dei Prodotti della Ricerca del Politecnico di Bari

Mechanical Characterization Of Carbon Fiber Reinforced Plastics Specimens For Aerospace Applications

This is a pre-print of the following article

Original Citation:
Mechanical Characterization Of Carbon Fiber Reinforced Plastics Specimens For Aerospace Applications / Barile, C.; Casavola, C.. - In: POLYMER COMPOSITES. - ISSN 0272-8397. - STAMPA. - 40:2(2019), pp. 716-722. [10.1002/pc.24723]

Availability:
This version is available at http://hdl.handle.net/11589/123186 since: 2022-06-22

Published version
DOI:10.1002/pc.24723

Publisher:

Terms of use:

(Article begins on next page)

02 May 2026

Mechanical characterization of Carbon Fiber Reinforced Plastics specimens for aerospace applications

C. Barile[1*], C. Casavola[1]

[1]Politecnico di Bari – Dipartimento di Meccanica Matematica e Management - Viale Japigia, 182 – 70126 BARI (Italy)

*Corresponding author: claudia.barile@poliba.it

Abstract

The use of new Composites Fibres Reinforced Plastics materials for structural applications in aerospace industry is fast increasing in the last years. Ensuring high performances requires a deep knowledge of the mechanical behaviour of the composite components subjected to different workloads. Components are subjected to strict environmental conditions that are typical of flight settings, as cold temperature and/or elevated temperature close to engines. In the typical assembly of composites, multiple layers are stacked together with a given sequence. Layers could be organized with different angles, different sequences and different technological process for providing specific mechanical properties that need to be studied. The possibility to introduce new parameters, able to improve mechanical properties of composites is also investigated. It refers to an unconventional fibres orientation combined with the through-the-thickness stitching on the in-plane mechanical properties of composites. Conventional carbon fibres orientation is generally referred to a Cartesian coordinate system, in which fibres are arranging in bundles along different angle orientations respect to the zero lamina. The opportunity to use a polar coordinate system of continue carbon tow is introduced to create specimens as well as complex geometry components easily. The application of this technique aims to introduce some advantages in the material's manufacturing process and if compared with the conventional strategy seems to be very promising since it appears to be very efficient in stopping delamination phenomenon.

Key words: composite material, mechanical properties, open hole, filled hole, RFI

1. INTRODUCTION

Carbon plastics reinforced with high-strength unidirectional fibers (CFRP) are composite materials that are increasingly used in various branches of engineering, especially for aerospace applications. The major advantage is connected to the higher performances respect to the metallic alloys [1-2]. This kind of materials consists, at least, of two separate phases which contributes together to the final properties: the reinforcement and the matrix. Differently from metallic materials, the "parts" of composites remain distinct from each other at the macroscopic level and are strongly affected by the delamination process of plies.

Different technological processes and lay-up distributions are continuously designed. The purpose is to obtain the maximum structural exploitation of fibers to meet the industrial requirements in terms of performances. The use of composite structures for aerospace applications has indicated an elevated level of complexity in mechanical design, due to the almost unlimited combinations of matrix and fiber patterns but also to the possibility of composites failing at loads not predictable neither by perfectly elastic nor perfectly plastic theories [3]. Thus, experimental tests continue to play a significant role in the qualification process for each new composite material by using traditional [4] or alternative techniques [5]. Aircraft structural design follows a pyramidal structure of testing, ranging from specimen tests to full-scale structure tests [6]. For this reason, it becomes important to plan a full experimental campaign that must consider several types of tests carried out at different temperatures, to simulate the real flight conditions. Anyway, to reduce

costs it could be advantageous to develop numerical analysis tools for predicting damages and failure, so that the amount of testing could be drastically reduced, and predictions could be made early in the design process.
Tensile and compression tests represent the main part of the qualification process for composite parts in aircraft structures. A consistent number of these type of tests are scheduled in a valid experimental campaign; they must provide response about the main mechanical properties at environmental conditions, at hot/wet temperatures as these of components close to the engines, and at cold temperatures as the real flight conditions. In general, the laws of deformation and failure of carbon fiber reinforced plastics (CFRP) at room and elevated temperatures are described adequately in many studies, generalized in handbooks and reviews [7-9]. For a more widespread application of such composites at cryogenic temperatures, for example, in cryogenic engineering or in open space, they must also be investigated under deep cooling conditions. Also joining process has a key role in the new composite's mechanical characterization. In fact, referring to joined composite components, mechanical fastening remains the primary means in modern aircraft structures, even though innovative approaches are now increasing in useful [10]. The stress concentration around the hole causes a considerable reduction in both the notched tensile and compressive strength of a composite laminate, that needs to be evaluated by experimental tests.
In this work, a combination of an experimental and numerical study is presented [11]. It is focused on different types of tensile and compression tests of composite material for aerospace applications. This paper aims to investigate the laws of deformation and failure of layered CFRP, reinforced with multidirectional fibers [12, 13], not only at room temperature, but also at low (-54°C) and high (71°C) temperatures [14-17]. Its purpose is to develop a numerical approach as support of traditional tests, able to estimate the mechanical properties of many CFRP materials only by varying some parameters in a simplified numerical model: percentage of each component, number of plies and fiber's orientation [18-20].
Materials has been produced by means of the Resin Film Infusion (RFI) and stitching process. Tensile and compression tests have been performed on specimens with three different lay-ups: 33/33/33, 40/40/20 and 100/0/0. They refer to the percentage of oriented fibers along three directions (0°/±45°/90°). Data observed are being used to develop a method for predicting the tensile and compression strength. Numerical results are compared with the experimental ones, aiming to define an innovative methodology adaptable to different case studies.

MATERIALS AND METHODS

Experimental campaign

Composite material analysed in this work has been realized by means of RFI and stitching process. The RFI process is faster, cheaper and capable of producing more complex components with better dimensional tolerances than the more traditional methods [21]. This should improve the use of composites in civil aviation and in aerospace field. Stitching process, instead, should improve the strength normal to the fibres direction, reducing delamination effects and buckling phenomena [22-27].
The material tested is composed by carbon fibres and epoxy matrix and it has been produced in sixteen tiles of specific configurations (Table 1).

Table 1. Data of tested materials.

Tile	Fibres Orientation %	No. Ply	Lay-up	Specimen Size [mm]	Ply thickness [mm]	Resin %
M1	33/33/33	12	$(0,45,90,-45,0,90)_s$	250x25	0.21	35.8
M2	33/33/33	12	$(0,45,90,-45,0,90)_s$	250x25	0.21	35.9
M4	33/33/33	12	$(0,45,90,-45,0,90)_s$	155x25	0.21	35.0
M5	33/33/33	12	$(0,45,90,-45,0,90)_s$	155x25	0.21	36.3
M6	33/33/33	12	$(0,45,90,-45,0,90)_s$	300x36	0.21	38.0
M7	33/33/33	12	$(0,45,90,-45,0,90)_s$	300x36	0.21	36.5
M8	33/33/33	12	$(0,45,90,-45,0,90)_s$	300x36	0.21	35.7
M9	33/33/33	12	$(0,45,90,-45,0,90)_s$	300x36	0.21	36.0
M18	40/40/20	10	$(0,45,90,-45,0)_s$	250x25	0.21	39.0
M19	40/40/20	10	$(0,45,90,-45,0)_s$	250x25	0.21	37.9
M22	40/40/20	20	$((0,45,90,-45,0)x2)_s$	155x25	0.21	33.0
M23	40/40/20	20	$((0,45,90,-45,0)x2)_s$	155x25	0.21	33.0
M24	100/0/0	4	(0,0,0,0)	250x15	0.20	40.0

M25	100/0/0	4	(0,0,0,0)	250x15	0.20	32.0
M26	100/0/0	14	14 times 0	155x10	0.21	34.0
M27	100/0/0	14	14 times 0	155x10	0.21	34.0

Three kinds of fibres orientation have been tested: 33/33/33, 40/40/20 and 100/0/0. Each number of the series refers to the percentage of fibres oriented along three directions: 0°/±45°/90° respect to the zero lamina, which is the fibres' direction of the top surface layer.

The specimens have been cut along three directions: 0°, 45° and 90° respect to the zero lamina. Each sample is identified by a code consisting of:

- "M" letter followed by the number of tile (M1, M2, etc.);
- sequence number of the specimen (M1_1, M1_2, etc.);
- orientation of the longitudinal axis of the specimen with respect to zero lamina (M1_1_0°, M2_1_90°, etc.).

This code allows to identify relation between the measured characteristics and the position of specimen into the tile considering edge's effect too.

Tests have been performed on 163 samples in order to define mechanical properties in different temperature conditions:

- Room Temperature (RT) in standard conditions at 23°C (79 specimens);
- Hot/Wet tests (HT) in climatic chamber at 71°C after a wet treatment for 15 days to simulate accelerated material's deterioration and real conditions close to engines (48 specimens);
- Cold tests (CT) in climatic chamber fed with liquid nitrogen up to -54°C, to simulate flight conditions (36 specimens).

The following tests were performed: tensile (T), open-hole tensile (TOH), filled-hole tensile (TFH), compression (C), open-hole compression (COH) and filled-hole compression (CFH). Tests were carried out in accordance with ASTM official standard [14, 28-32]. Table 2 summarizes the experimental plan. At least three specimens are investigated for each type of test.

Table 2. Experimental plan for 0° and 90° specimens' orientation.

	0 deg				**90 deg**				
Type of test	**Tile**	**CT**	**RT**	**HT**	**Tile**	**CT**	**RT**	**HT**	**Tot.**
T	**M1**	3	3	3	**M2**	3	6	3	21
T	**M24**	3	3	3	**M25**	3	6	3	21
T	**M18**	3	4	3	**M19**	3	6	3	22
TOH	**M6**		3						3
TFH	**M7**	3	3		**M8**	3	3		12
C	**M4**	3	6	3	**M5**		6	3	21
C	**M26**	3	3	3	**M27**	3	6	3	21
C	**M22**	3	3	3	**M23**		6	3	18
COH	**M6**		3	3	**M9**		3	3	12
CFH	**M7**		3	3	**M8**		3	3	12

The experimental tests were performed on a servo-hydraulic testing machine having 100 kN capacity at a quasi-static rate, in displacement control. Strains were acquired by electrical strain gages or extensometers attached to the mid-section of the specimens for a direct comparison with finite-element models. In addition, a climatic chamber has been used for realizing both the hot and cold tests.

For each tested specimen, the longitudinal elasticity modulus E and the ultimate strength σ_u have been calculated. The modulus E has been evaluated, as the slope of the elastic trend of the stress-strain curve far from fracture zone. The ultimate strength has been estimated as the ratio between the ultimate load and the resistant cross-section, disregarding hole in specimens for TOH, TFO, COH, CFH. At the end of each test, location and mode of failure of the specimen were analyzed and classified as suggested in [14, 28-32]. Figure 1 reports the set up for tensile test at cold temperature, for compression at room temperature and for compression open hole tests at hot temperature.

Figure 1. Set up for tensile, compression and compression filled hole tests.

Numerical model

In order to simulate tensile and compression tests, a finite element model was developed using the commercial software ANSYS® 14.5. Shape, dimensions, number of layers, percentage of fibers orientation and lay-ups of each specimen were modeled. The elastic properties used during simulation were experimentally evaluated. They are:

- E_x, the elastic modulus of specimen with 100% of fibers along the load direction.
- E_y, the elastic modulus of specimen with 0% of fibers along the load direction.
- G_{xy}, evaluated testing unidirectional specimens cut at 45° respect to the fibers' direction and recording the strains along the fibers ($\varepsilon_{45°}$) and perpendicularly to the fibers ($\varepsilon^*_{45°}$).

$$G_{xy} = \frac{\tau_{xy}}{\gamma_{xy}}$$

where

$$\tau_{xy} = \frac{P}{2ab}$$

and

$$\gamma_{xy} = \varepsilon_{45°} - \varepsilon^*_{45°}$$

P is the load applied and ab is the specimen's cross section.

ν_{yx}, calculated testing unidirectional specimens cut at 90° respect to the zero lamina and recording the strains in the longitudinal (ε_y) and transverse (ε_{yx}) directions:

$$\nu_{yx} = \frac{\varepsilon_{yx}}{\varepsilon_y}$$

The load applied was characteristic of each specimen and is evaluated in correspondence of a strain of 3000 με.

The specimen material was modeled assuming each layer as an orthotropic material. This modeling choice was justified since each ply has fibers in only one direction. This analysis was carried out to define a numerical model that good represents the experimental one, aiming to reduce the tests numbers.

The mesh included 6250 elements and 19301 nodes (Figure 2).

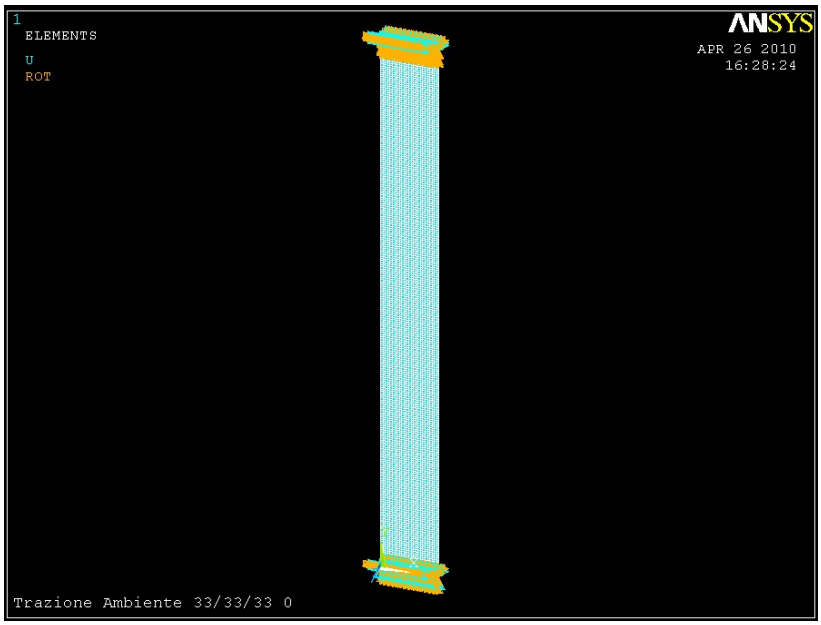

Figure 2. Finite element model of the tensile test simulated numerically.

RESULTS

Experimental campaign

Values of stress and strain have been recorded during all experimental tests. At least three replications were performed for each lay-up.

Table 3 lists the mean values of ultimate strength and longitudinal modulus obtained from tensile tests at the three temperatures (Room, Hot and Cold Temperature). For each tile, it can be observed that generally the ultimate strength is almost comparable in all three temperatures. Regarding the modulus of elasticity instead, at CT it is approximately twice that at HT and RT, since epoxy matrix are inclined to become brittle at cold temperatures. It seems that composite material behavior has been mostly affected by the fibers, which have very high thermal stability if compared with traditional metal materials.

Table 3. Experimental results for tensile tests (T) at different temperatures and different lay-up.

	HT		**CT**		**RT**	
Tile	**Ultimate strength [MPa]**	**Modulus of elasticity [MPa]**	**Ultimate strength [MPa]**	**Modulus of elasticity [MPa]**	**Ultimate strength [MPa]**	**Modulus of elasticity [MPa]**
M1_0°	605	54033	637	109767	540	52300
M2_90°	496	51700	545	105633	538	54217
M18_0°	1016	85733	748	137600	830	71125
M19_90°	605	45900	509	84333	555	43567
M24_0°	789	155200	767	213067	1409	277900
M25_90°	27	5100	31	14767	43	5640

Figure 3 shows the results of tensile tests at HT obtained for different fibers orientation: 33/33/33, 40/40/20, 100/0/0. M1 and M2 tiles (33/33/33) present the identical performance both for 0° and 90° samples; M24 and M25 tiles (100/0/0) exhibit respectively the highest and lowest slope of the stress-strain curve; M18 and M19 tiles (40/40/20) show a middle tendency. This trend is representative for all three experimental temperatures.

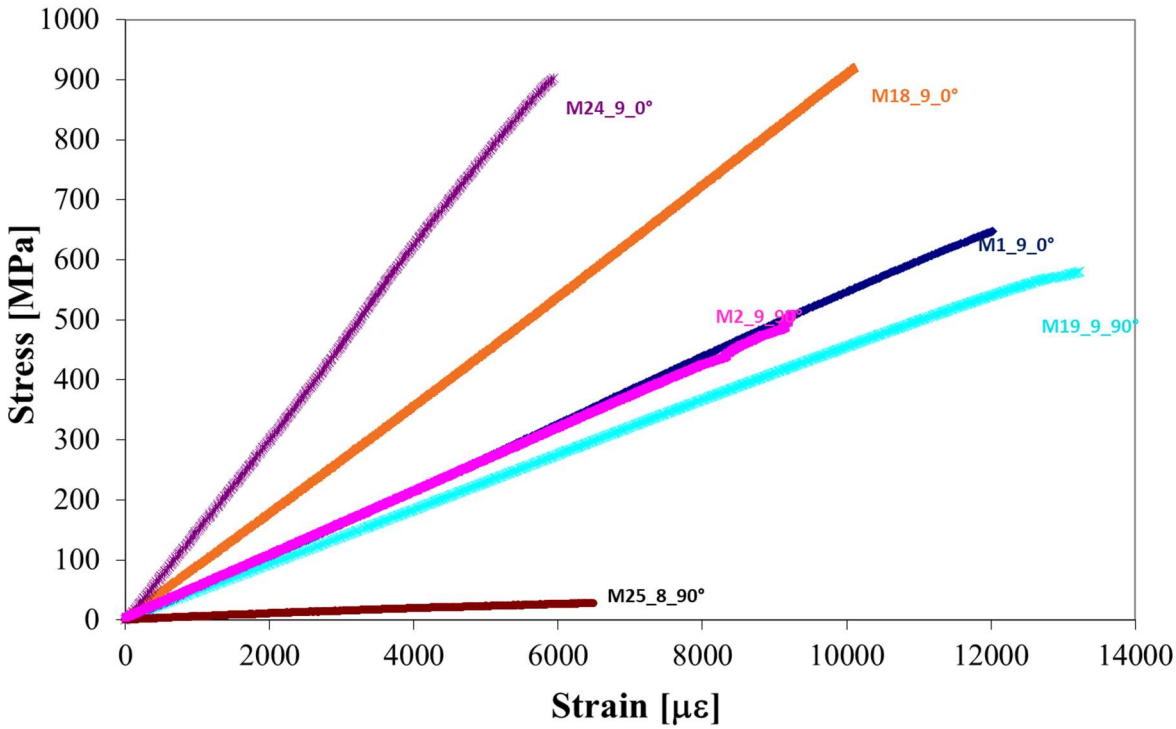

Figure 3. Tensile tests results obtained at HT for different lay-up of tiles.

Table 4 reports the mean values of ultimate strength and longitudinal elasticity modulus obtained for compression tests at the three temperatures (Room, Hot and Cold Temperature). In this case, it can be observed that, for each tile, the elasticity modulus at CT are mostly like those at RT and HT. The ultimate strength increases in absolute value at CT.

Table 4. Experimental results for compressive tests (C) at different temperatures and different lay-up.

	HT		CT		RT	
Tile	**Ultimate strength [MPa]**	**Modulus of elasticity [MPa]**	**Ultimate strength [MPa]**	**Modulus of elasticity [MPa]**	**Ultimate strength [MPa]**	**Modulus of elasticity [MPa]**
M4_0°	-294	49300	-360	49533	-311	45717
M5_90°	-248	54300	-306	54700	-198	55250
M22_0°	-274	66500	-430	56800	-305	58533
M23_90°	-241	43533	-330	42900	-257	40617
M26_0°	-463	122300	-612	115600	-504	115200
M27_90°	-138	7800	-216	9950	-110	7000

Figure 4 shows the results of compression tests obtained at HT for different fibers orientation: M4 and M5 (33/33/33) show the same behavior both for 0° and 90° specimens; M26 and M27 (100/0/0) show respectively the highest and lowest slope; M22 and M23 (40/40/20) show an intermediate trend. As for tensile tests, this graph is representative for all three experimental temperatures.

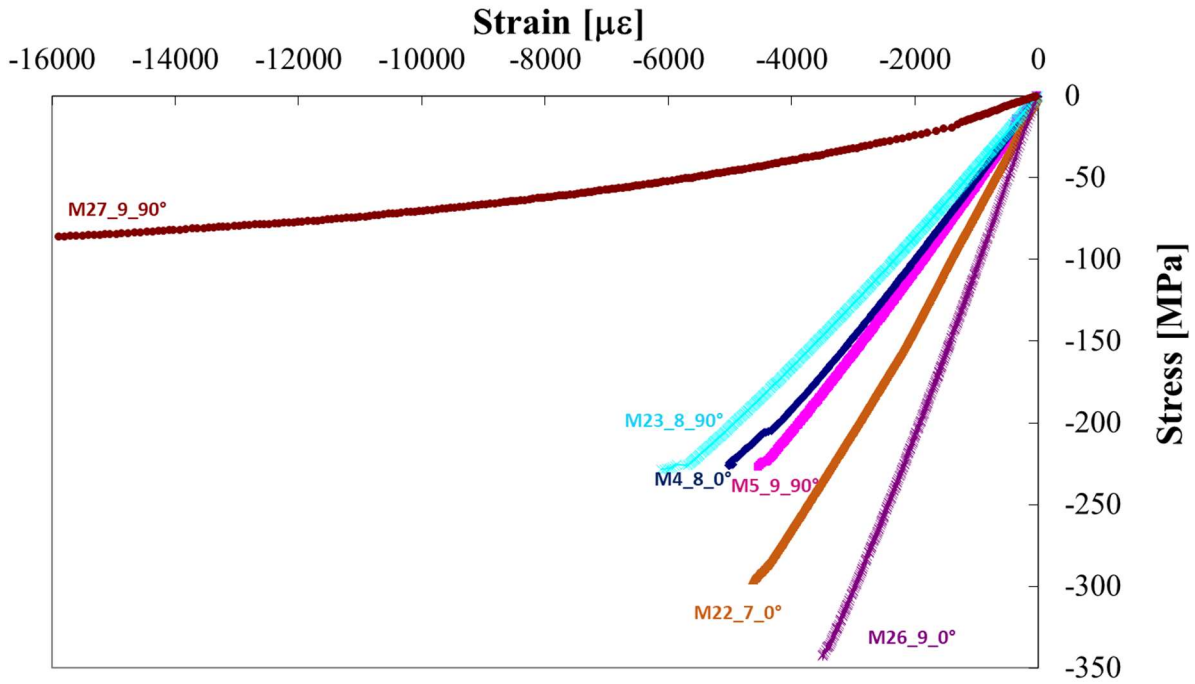

Figure 4. Compression tests results obtained at HT for different lay-up of tiles.

Table 5 compares mean values of mechanical properties carried out according different kind of tests: tensile (T, TOH and TFH) and compressive (C, COH and CFH) at RT. The existence of fastener increases the ultimate strength in TFH tests of about 14% whit respect to TOH test. On the contrary, the hole reduces the strength of about 25% whit respect to T test. An analogous behavior is observed in compression tests.

Table 5. Experimental results for tensile and compression tests on unnotched, open hole and filled hole specimens.

Tile	M1_0°_T	M6_0°_TOH	M7_0°_TFH	M4_0°_C	M6_0°_COH	M7_0°_CFH
Ultimate strength [MPa]	540	402	465	-311	-255	-286

Figure 5 shows the post-failure state of each type of test. All samples failed in accordance with the acceptable failure modes set out in ASTM Standard [14, 28-32]. The ultimate failure occurred in all specimens almost instantaneously, with little warning few seconds before the ultimate failure: some “pings”, typical of fiber failure, and harsh tearing sounds, characteristic of delamination, heard.

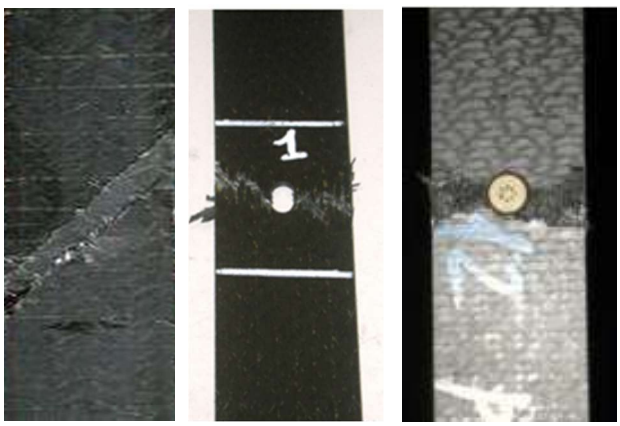

Figure5. Typical fracture for tensile, tensile open hole and filled hole.

Figure6. Typical fracture for compression, compression open hole and filled hole.

Numerical model

Tables 6 and 7 summarize results of tiles experimentally tested and numerically modeled. They report the percentage error evaluated as follows:

$$E = \frac{\varepsilon_{simulated} \quad \varepsilon_{experimental}}{\varepsilon_{experimental}} * 100$$

The percentage errors are all positive, indicating that numerical results are bigger than the experimental ones. This attitude confirms the difficulties in modelling the stitched points, whose presence deeply affects the composite behavior. It can also be underlined that the compression errors are larger than the tensile ones, demonstrating the more influent effects of the stitching for this kind of test [22-27].

Another interesting observation refer to the errors for 40/40/20 tiles. They are higher than the other ones.

Finally, it can be observed that the errors for 0° specimens are lower than 90° ones.

Table 6. Tensile percentage errors between numerical and experimental results.

Tile	Deg	Fibres Orientation %	No. Ply	Lay-up	Error %
M1	0°	33/33/33	12	(0,45,90,-45,0,90)s	+ 10,63
M2	90°	33/33/33	12	(0,45,90,-45,0,90)s	+ 15,95
M18	0°	40/40/20	10	(0,45,90,-45,0)s	+ 17,62
M19	90°	40/40/20	10	(0,45,90,-45,0)s	+ 10,74
M24	0°	100/0/0	4	(0,0,0,0)	+ 9,74
M25	90°	100/0/0	4	(0,0,0,0)	+ 13,08

Table 7. Compressive percentage errors between numerical and experimental results.

Tile	Deg	Fibres Orientation %	No. Ply	Lay-up	Error %
M4	0	33/33/33	12	$(0,45,90,-45,0,90)_s$	+ 19,41
M5	90	33/33/33	12	$(0,45,90,-45,0,90)_s$	+ 10,12
M22	0	40/40/20	20	$(0,45,90,-45,0)_s$	+ 15,93
M23	90	40/40/20	20	$(0,45,90,-45,0)_s$	+ 17,78
M26	0	100/0/0	14	14 times 0	+ 15,96
M27	90	100/0/0	14	14 times 0	+10,54

CONCLUSIONS

In the present work a study on high-strength carbon/epoxy composite obtained by means of stitching and resin film infusion was done. Three significantly different lay-ups have been tested and modeled.

Experimental tensile and compression tests have been performed at room temperature, at hot/wet and at cold conditions, in order to characterize mechanical properties of material in different working conditions. Unnotched, open hole and filled hole specimens have been considered too.

Experimental data suggest the several observations:

- Tensile and compressive mechanical properties tend to increase by reducing temperature; it could be linked to the carbon fibers behavior thermal stability.
- The hole introduces a discontinuity in fibers and a localized defect due to the drilling operation; it affects the composite material behavior, but in this case the plies have been stitched together reducing delamination.
- Mechanical properties decrease in the case of drilled specimens of about 20%, but the fastener presence cooperates in reducing this effect.

The deformations predicted from the FEM analysis has been shown to be bigger than the experimental ones because the composite behavior is sensitive to the stitching procedure and the stitched points are difficult to represent correctly in the model. In addition, the compressive numerical results indicate that stitching has a beneficial effect especially on the compression strength. Through-thickness stitching followed by RFI process is one of the most promising and cost-effective methods of manufacturing composite structures with higher delamination resistance.

Referring to numerical models, future works will involve different type of load, lay-ups and geometries in order to really realize the possibility of saving both experimental costs and time.

REFERENCES

[1] S.T. Peters, *Handbook of composite*s, Chapman & Hall (1998).

[2] L. Tong, A. P. Mouritz, M. K. Bannister. *3D fiber reinforced polymer composites*. Ed. Elsevier (2002).

[3] N. K Kucher, M. P. Zemtsov, and M. N. Zarazovskii, *Mech. Compos. Mater.*, **42**, 5:407-418 (2006).

[4] C. Barile, C. Casavola and C. Pappalettere, *Composites Part B*, **110**, 248-254 (2017).

[5] C. Barile, C. Casavola, G. Pappalettera and C. Pappalettere, Conference Proceedings of the Society for Experimental Mechanics Series, **66**, 5:247-252 (2015).

[6] R. M. O'Higgins, G. S. Padhi and M. A. McCarthy, C. T. McCarthy. Experimental and numerical study of the open-hole tensile strength of carbon/epoxy composites. *Mech. Compos. Mater.*, **40**, 4:269-278 (2004).

[7] B. Cox and G. Flanagan, *Hanbook of analytical methods for textile composites*, NASA Contractor Report 4750. Langley Research Center (1997).

[8] W. J. Cantwell and J. Morton, *Compos.* **22** 347–362 (1991).

[9] A. P. Mouritz, K. H. Leong and I. Herszberg, *Compos Part A* **28**A 979–991 (1997).

[10] C. Wang, P. Uawongsuwan, H. Mori, Y. Yang, A. Nakai, H. Hamada, Proceedings of the 28th Annual Technical Conference of the American Society for Composites 2013, State College, Pennsylvania, USA, 9-11 September 2013, 437-443.

[11] H. Fan, A.P. Vassilopoulos and T. Keller, *Comp Part B* **91** 327–336 (2016).

[12] A. Barchan and R. Chatys, *Mech. Compos. Mater.* **44**, 2:131-138 (2008).

[13] E. Sparnins, J. Andersons, Modeling the nonlinear deformation of composite laminates based on plasticity theory. *Mech. Compos. Mater.,* **43**, 3:203-210 (2007).

[14] ASTM D 5229/D 5229M. Standard Test Methods for Moisture Absorption Properties and Equilibrium Conditioning of Polymer Matrix Composite Materials. Marzo 2004.

[15] I. Kafodya, G. Xian and H. Li, *Comp Part B* **70** 138–148 (2015).

[16] Y. Ou, D. Zhu, H. Hang, Y. Yao, B. Mobasher and L. Huang, *Comp Part B* **95** 123–136 (2016).

[17] A. Zhou, L. Tam, Z. Yu and D. Laumia, *Comp Part B* **71** 63–73 (2015).

[18] S. Kobayashi, J. Kitagawa, *Comp Part B* **85** 31–40 (2016).

[19] E. G. Koricho, G. Belingardi, *Comp Part B* **79** 430–443 (2015).

[20] Y. Zheng, X. Cheng and B. Yasir, *Chin J Aeronaut* **25** 473–484 (2012).

[21] N. L. Han, S. S. Suh, J. M. Yang, H. T. Hahn, *Composites Part A,* **34**, 3 227–236 (2003).

[22] K. A. Dransfield, L. K. Jain and Y. W. Mai, *Compos Sci Technol,* **58,** 6 815–827 (1998).

[23] F. Aymerich and P. Priolo, *Int J Impact Eng,* **35** 591–608 (2008).

[24] K. Dransfield, C. Baillie and Y.W. Mai, *Compos Sci Technol,* **50**, 3 305–317 (1994).

[25] A. Yudhanto, N. Watanabe, Y. Iwahori, H. Hoshi, *Comp Part B,* **46** 151–165 (2013).

[26] A. Yudhanto, N. Watanable, Y. Iwahori and H. Hoshi, *Compos Part B*, **46** 151–165 (2013).

[27] A. Yudhanto, N. Watanable, Y. Iwahori and H. Hoshi, *Mater Des* **35** 563–571(2012).

[28] ASTM D 3039/D 3039M. Standard Test Method for Tensile Properties of Polymer Matrix Composite Material. Luglio 2000.

[29] ASTM D 5766/D 5766M. Standard Test Method for Open Hole Tensile Strength of Polymer Matrix Composite Laminates. Febbraio 2003.
[30] ASTM D 6742/D 6742M. Standard Practice for Filled-Hole Tension and Compression Testing of Polymer Matrix Composite Laminates. Novembre 2002.
[31] ASTM D 3410/D 3410M. Standard Test Method for Compressive Properties of Polymer Matrix Composite Materials with Unsupported Gage Section by Shear Loading. Agosto 2003.
[32] ASTM D 6484/D 6484M. Standard Test Method for Open-Hole Compressive Strength of Polymer Matrix Composite Laminates. Aprile 2004.